Howard Hughes Medical Institute

Published as: *Clin Cancer Res*. 2019 December 15; 25(24): 7554–7564.

Interleukin-15 Enhances Anti-GD2 Antibody-Mediated Cytotoxicity in an Orthotopic PDX Model of Neuroblastoma

Rosa Nguyen[1], **Ardiana Moustaki**[2], **Jacqueline L. Norrie**[3], **Shantel Brown**[4], **Walter J. Akers**[4], **Abbas Shirinifard**[3], **Michael A. Dyer**[3]

[1]Department of Oncology, St. Jude Children's Research Hospital, Memphis, Tennessee

[2]Department of Immunology, St. Jude Children's Research Hospital, Memphis, Tennessee

[3]Developmental Neurobiology, St. Jude Children's Research Hospital, Memphis, Tennessee

[4]Center for In Vivo Imaging and Therapeutics (CIVIT), St. Jude Children's Research Hospital, Memphis, Tennessee

Abstract

Purpose: Immunotherapy with interleukin (IL)-2, granulocyte-macrophage colony-stimulating factor (GM-CSF), and an anti-disialoganglioside (GD2) antibody significantly increases event-free survival in children with high-risk neuroblastoma. However, therapy failure in one-third of these patients and IL-2–related toxicities pose a major challenge. We compared the immunoadjuvant effects of IL-15 with those of IL-2 for enhancing antibody-dependent cell-mediated cytotoxicity (ADCC) in neuroblastoma.

Experimental Design: We tested ADCC against neuroblastoma patient-derived xenografts (PDXs) *in vitro* and *in vivo* and examined the functional and migratory properties of NK cells activated with IL-2 and IL-15.

Results: In cell culture, IL-15–activated NK cells induced higher ADCC against two GD^+ neuroblastoma PDXs than did IL-2–activated NK cells ($P < 0.001$). This effect was dose-dependent ($P < 0.001$) and was maintained across several effector-to-tumor ratios. As compared with IL-2, IL-15 also improved chemotaxis of NK cells, leading to higher numbers of tumorsphere-infiltrating NK cells *in vitro* ($P = 0.002$). In an orthotopic PDX model, animals receiving chemoimmunotherapy with an anti-GD2 antibody, GM-CSF, and a soluble IL-15/IL-15Rα complex had greater tumor regression than did those receiving chemotherapy alone ($P = 0.012$) or combined with anti-GD2 antibody and GM-CSF with ($P = 0.016$) or without IL-2 ($P = 0.035$). This was most likely due to lower numbers of immature tumor-infiltrating NK cells ($DX5^+CD27^+$) after IL-15/IL-15Rα administration ($P = 0.029$) and transcriptional upregulation of *Gzmd*.

Conclusion: The substitution of IL-15 for IL-2 leads to significant tumor regression *in vitro* and *in vivo* and supports clinical testing of IL-15 for immunotherapy in pediatric neuroblastoma.

Corresponding author: Michael A. Dyer, 262 Danny Thomas Place, Memphis, TN 38105, USA. Phone: 901-595-2257; Fax: 901-521-7641; michael.dyer@stjude.org.

Conflict of interest disclosure: The authors have no disclosures.

Keywords

Interleukin 15; NK cells; neuroblastoma; immunotherapy; pediatric oncology

Introduction

Neuroblastoma is the most common extracranial solid tumor of childhood (1). Most children present with high-risk disease, of which only half are cured with conventional chemotherapy, surgery, and radiation therapy (1, 2). However, the addition of immunotherapy with interleukin (IL)-2, granulocyte-macrophage colony-stimulating factor (GM-CSF), an anti-disialoganglioside (GD2) antibody combined with *cis*-retinoic acid significantly extends event-free survival in these patients and is now the standard of care (3). Despite this achievement, one-third of children experience treatment failure while receiving immunotherapy or are unable to tolerate IL-2–related side effects (2, 4). Improving the current immunotherapeutic regimen is therefore important to maximize survival and decrease therapy-related toxicities.

Anti-GD2 antibodies mediate tumor-directed therapeutic effects through antibody-dependent cell-mediated cytotoxicity (ADCC), for which natural killer (NK) cells are the primary effector cells that bind to the F_c portion of the antibody and eliminate antibody-labeled tumor cells (5). IL-2 is a stimulatory cytokine and increases the cytotoxic capacity of NK cells by engaging the IL2 receptor βγ (IL2Rβγ), which is constitutively expressed on the cell surface of NK cells. In addition to IL-2, other cytokines such as IL-15 can bind to IL2Rβγ and induce overlapping biologic effects *in vivo* (6).

Preclinical studies established the importance of IL-15 on NK cell maturation and function (7–9). More recently, clinical development of recombinant human IL-15 determined tolerability in adults and elucidated the biologic effects of IL-15 and NK cell homeostasis in humans. In patients receiving recombinant human IL-15, NK cells hyperproliferate and attain an activated phenotype, leading to NK cell expansion *in vivo* and tumor shrinkage in two patients (10). Because NK cells are one of the main effector cells of ADCC (5), we hypothesize that IL-15 is equally or potentially more efficient than IL-2 in enhancing NK cell–mediated ADCC against neuroblastoma. Therefore, to compare the immunoadjuvant effects of IL-15 versus IL-2, we performed ADCC studies in culture and *in vivo*, contrasting the specific lysis of neuroblastoma patient-derived xenografts (PDXs) by IL-2– and IL-15–activated NK cells. In addition, we examined the cellular properties of IL-2– and IL-15–activated NK cells and quantified their ability to induce tumor cell death and infiltrate tumorspheres. Altogether, our studies demonstrate that IL-15 is more effective than IL-2 to enhance ADCC against neuroblastoma and support our current efforts to develop a clinical trial to test the efficacy of IL-15 for immunotherapy in pediatric neuroblastoma.

Materials and Methods

Tumor cells

Neuroblastoma cell lines were maintained in RPMI 1640 medium (Lonza; CHLA90; ATCC) and DMEM (Lonza; SK-NAS; ATCC) supplemented with 10% heat-inactivated fetal bovine serum (Biowest), 100 IU/mL of penicillin, 100 μg/mL of streptomycin, and 2 mM of L-glutamine (all Gibco media). Cells tested negative for mycoplasma by PCR, and short tandem repeat profile confirmed their identity when they were frozen as batches of 20 vials. After thawing, cells were passaged for at least 5 passages and then used for experiments. New cells were retrieved from the same cryobatch every 2 months after thawing. The PDX lines SJNBL108_X and SJNBL047443_X1 were grown orthotopically in CD1-*Foxn1*^{nu} immunodeficient mice (Charles River Laboratories). Karyotype analysis of SJNBL046_X revealed gain on chromosome 17 by fusion to chromosomes 13 and 22, gain on chromosome 1 by fusion to chromosome 7, and gain on chromosome 7 and 15 by fusion to chromosome 1. *MYCN* amplification was confirmed by fluorescence in situ hybridization (11). All animal studies were approved by the Institutional Animal Care and Use Committee of St. Jude Children's Research Hospital. Palpable tumors were harvested and processed into single-cell suspensions for *ex vivo* testing (5).

Animals and orthotopic tumor injections

CD1-*Foxn1*^{nu} mice were used for *in vivo* immunotherapy testing. We visualized the injection area by using a VEVO 2100 high-frequency ultrasound instrument (Fujifilm Visualsonics) with an MS-700 transducer (50 MHz). Under anesthesia with isoflurane, mice aged 5 to 6 weeks received para-adrenal injections of PDX cells, which were resuspended as a single-cell solution in Matrigel (Corning Inc.), as previously described (11). As previously described, SJNBL046_X tumors grow orthotopically within 4-6 weeks from implantation date (11).

Human NK cell preparation and culture

Human NK cells were isolated from residual peripheral blood from heparinized apheresis rings obtained from healthy deidentified donors. Each *in vitro* experiment was performed with fresh NK cells from a new donor. Peripheral blood mononuclear cells were isolated via density-gradient centrifugation with Ficoll-Paque Plus (GE Healthcare). Red cell lysis was performed with lysis buffer (Qiagen). The RosetteSep Human NK Cell Enrichment Cocktail (Stem Cell Technologies) and human MACSxpress NK Cell Isolation Kit (Miltenyi Biotec) were used to isolate NK cells with a purity of >95%. RPMI-based media supplemented with 10% heat-inactivated fetal bovine serum, 100 IU/mL of penicillin, 100 μg/mL of streptomycin, and 2 mM of L-glutamine (all Gibco media) was used to grow NK cells in *ex vivo* cultures. IL-2 (50 IU/mL) and IL-15 (10 ng/mL) were provided by the Biological Resource Branch at the National Cancer Institute for preactivation of NK cells in culture.

Monoclonal therapeutic antibodies

The anti-GD2 antibody hu14.18K322A (humanized anti-human) was provided to St. Jude Children's Research Hospital and Children's GMP, LLC (Memphis, TN) by Merck Serono

(Darmstadt, Germany) and was manufactured by Children's GMP, LLC. Hu14.18K322A was used in all *in vitro* ADCC experiments because it recognizes human GD2 and contains a human F_c portion that is recognizable by human NK cells. In *in vivo* experiments, the monoclonal antibody 14.G2a (mouse anti-human) provided by the Biological Resource Branch at the National Cancer Institute was used because it recognizes human GD2 but contains a murine F_c portion.

ADCC and NK cytotoxicity assays

For ADCC assays, PDX were dissociated into a single-cell suspension and grown in culture in 96-well flat-bottom plates (Corning Inc.) at 37° in 5% CO_2 incubators for 24 hours prior to the experiment. To induce ADCC, hu14.18K322A (10 μg/mL) was added to culture wells 1 hour before coincubating effector cells with tumor cells. The duration of the ADCC assay was 12 hours. The ADCC assays were performed with effector-to-target (E:T) cell ratios ranging from 1:5 to 1:1.25. The CellTiter-Glo luminescent cell viability assay (Promega) was used according to manufacturer instructions to quantify specific lysis. A plate reader (SpectraMax M3) measured the luminescence in relative light units (RLU), and specific lysis was calculated with the following formula: specific lysis (%) = $(1 - \frac{\text{RLU treated} - \text{RLU untreated}}{\text{RLU untreated}}) \times 100$.

To test natural NK cell cytotoxicity (i.e., cytotoxicity in the absence of antibody), the experimental set-up and quantification were identical to the ADCC assays; however, no hu14.18K322A was added.

Two-dimensional cell colocalization assay

One day before the assay, NK cells were grown in culture in NK cell media supplemented with IL-2 (50 IU/mL) or IL-15 (10 ng/mL) for 12 to 18 hours, and neuroblastoma cells were plated at a density of 50,000 cells per well in 4-well glass bottom chamber slides (Ibidi). On the day of the assay, neuroblastoma cells were labeled with calcein-AM, and NK cells were labeled with CellTracker Orange (Thermo Fisher Scientific), according to manufacturer instructions. Hu14.18K322A (10 μg/mL) was added to the wells for 1 hour to allow binding to tumor cells. Dye-labeled NK cells were then added to the wells containing neuroblastoma cells. A C2 Nikon confocal microscope (Nikon) was used to perform live-cell imaging at a magnitude of 10X for 12 hours. Five different areas were imaged per condition. To quantify the imaging data, we extracted the green (8 bit) and red (16 bit) channels and segmented the green and red signal with FIJI software (12) and Weka Trainable Segmentation plug-in (13). We converted the segmented images into a binary mask and applied the 3D ROI manager plug-in to calculate contact area in μm and signal intensity (14).

Tumorsphere formation and 3-dimensional infiltration assay

Yellow fluorescent protein (YFP)-expressing PDX tumors were processed into single-cell suspensions and resuspended in Dulbecco modified eagle medium (Lonza) supplemented with 10% heat-inactivated fetal bovine serum, 100 IU/mL penicillin, 100 μg/mL streptomycin, and 10 μM rho kinase pathway inhibitor Y-27632 (Stem Cell Technologies). Tumor cells were plated at a density of 50,000 cells per well into 96-well low-attachment

round-bottom plates (Lipidure), centrifuged at 100 × *g* for 5 minutes, and maintained at 37° in 5% CO2 incubators. On day 3 after plating, single tumorspheres were transferred into 24-well low-attachment plates (Thermo Fischer Scientific) and grown for 24 to 48 hours. To determine NK cell infiltration into the tumorspheres, NK cells were labeled with CellTracker Orange, as per manufacturer instructions. NK cells were coincubated with tumorspheres at an E:T ratio of 5:1 for 12 hours. The tumorspheres were then fixed with 4% paraformaldehyde for 2 hours and placed in 30% sucrose. Cryosections (8 micron thickness) were stained with 4′,6-diamidino-2-phenylindole and imaged with a C2 Nikon confocal microscope. Tumorsphere-infiltrating NK cells were counted for each section, and results were normalized by the sectioned area. To assess cytotoxicity, NK cells isolated by fluorescence-activated cell sorting (FACS) from tumorspheres were tested against K562 for 4 hours. The E:T ratio was 5:1. Residual tumor cells were quantitated by flow cytometry and the results were normalized with particles for absolute cell counting (Spherotech).

IL-15/IL15-Rα precomplexing

Precomplexing of IL-15/IL-15Rα was performed with recombinant mouse IL-15 (Peprotech) and mouse IL-15Rα Fc chimera (R&D) by incubating 2.5 μg of IL-15 and 12 μg of IL-15Rα at room temperature for 30 minutes as previously described (15).

In vivo immunotherapy testing

All *in vivo* testing was performed with tumor-bearing mice with tumor volumes measuring ≥10 mm^3 by ultrasound (i.e., an established tumor model). Animals were randomized to four therapy groups: chemotherapy alone (group 1); chemotherapy followed by anti-GD2 antibody and GM-CSF (group 2); chemotherapy followed by anti-GD2 antibody, GM-CSF, and IL-2 (group 3); chemotherapy followed by anti-GD2 antibody, GM-CSF, and IL-15/IL-15Rα complex (group 4). Chemotherapy was given during week 1 of each cycle and consisted of daily intraperitoneal injections of irinotecan (1.6 mg/kg) and oral administration of temozolomide (16.5 mg/kg) for 5 days. All animals in groups 2, 3, and 4 received 100 μg of the mouse anti-human 14.G2a anti-GD2 antibody on days 2 through 5 of week 2. Animals assigned to group 2 received daily 50 μg/kg of intraperitoneal murine GM-CSF for 5 days of week 2. Mice in group 3 were given daily 10,000 IU of recombinant mouse IL-2 (Peprotech) intraperitoneally and daily murine GM-CSF for 5 days of week 2. The mouse IL-15/IL-15Rα complex was administered intraperitoneally to group 4 mice on day 1 of week 2 together with murine GM-CSF. Each therapy cycle lasted for 3 weeks and a total of two cycles were administered to animals. Staff specialized in preclinical imaging were blinded to the therapy groups and conducted weekly acquisition of the index lesions with a VEVO 2100 high-frequency ultrasound instrument (S.B.) and tumor volume measurements with VEVO LAB software, version 3.1.1 (W.J.A).

Flow cytometry and FACS

NK cell purity after isolation was determined by flow cytometry and defined as $CD3^-$ (UCHT1) and $CD56^+$ cells (NCAM16.2; BD). For phenotypic analysis of murine immune cells, the following antibodies were used: Cd11c (N418), Cd49b (DX5), Ly-6C (1A8), Ly-6G (HK1.4), MHC II (M5/114.15.2; all Biolegend), B220 (RA3-6B2; Tonbo Bioscience), Cd45 (30-F11), Cd11b (M1/70), Cd27 (LG 3A10; all BD Biosciences). For

blocking, the purified human FcR binding inhibitor (Thermo Fisher) and anti-mouse CD16/CD32 (2.4G2; Tonbo Bioscience, San Diego, CA) were used. Data were acquired with a BD Biosciences Fortessa instrument with four-laser capacity (17 colors) and analyzed with FCS Express, version 6.

Statistical analysis

We used D'Agostino-Pearson omnibus and Shapiro-Wilk normality tests to determine normal distributions of variables. Normally distributed groups were compared with two-tailed Student *t* tests for paired and unpaired data (two groups) and one-way analysis of variance and Tukey multiple comparison tests for post-hoc analysis of multiple groups. If data were not normally distributed, we log-transformed the data and used parametric tests. Alternatively, we used unpaired Mann-Whitney tests (two groups) and unpaired Kruskal-Wallis tests with Dunn post-hoc analysis of multiple comparisons for nontransformed non-normally distributed data. Parametric Pearson tests were used for correlation analysis. Linear regression analyses were performed for continuous dependent variables. All statistical analyses were conducted with GraphPad Prism 8 or JMP, version 14 (linear regression analysis). P values < 0.05 were considered statistically significant.

Results

IL-15 enhances NK cell-mediated ADCC against GD2$^+$ neuroblastoma *in vitro*

To compare the immunoadjuvant effect of IL-2 with that of IL-15 on NK cell–mediated lysis of neuroblastoma cells in culture, we preactivated NK cells with decreasing concentrations of IL-2 (1–50 IU/mL) and IL-15 (1–10 ng/mL) for 24 hours. These concentrations were chosen because they correspond approximately to steady-state levels in humans treated with less than or equivalent to the maximum tolerated doses of IL-2 (4) and IL-15 (10). We then added preactivated NK cells to cocultures with the PDX SJNBL046_X at multiple E:T ratios for 12 hours and found that the cytotoxic activity of NK cells was higher after preactivation with IL-15 than with IL-2 ($P < 0.001$; Fig. 1A). This effect occurred in a dose-dependent manner ($P < 0.001$) and was maintained with lower cytokine doses and E:T ratios. When we analyzed the E:T ratios, we observed that higher tumor lysis by IL-15–activated NK cells was dependent on cytokine concentration ($P < 0.05$).

To confirm these findings, we extended our *in vitro* testing to include four donors and two PDX lines, SJNBL046_X and the *ATRX*-mutant line SJNBL047443_X1. NK cells were grown in culture in the presence or absence of intermediate doses of IL-2 (i.e., 10 IU/mL) or IL-15 (i.e., 5 ng/mL), and an E:T ratio of 5:1 was used in the assay. When we performed multiple comparisons of the cytotoxic activity of resting and IL-2– and IL-15–stimulated NK cells among donors and PDX lines, we found that the most effective tumor cell ablation was achieved by IL-15–activated NK cells (Fig. 1B and C). Specific lysis was dependent on the type of cytokine used to induce activation ($P < 0.001$) and the presence of hu14.18K322A ($P < 0.001$). Altogether, these results show that the stimulatory effect of IL-15 exceeded that of IL-2 and led to improved ADCC against neuroblastoma PDX cells in culture.

Tumor and NK cell contact is enhanced by IL-2 and IL-15 stimulation

Because IL-15 can alter chemotaxis and adhesion properties of NK cells (16, 17), we compared the cellular interactions of NK cells with tumors after IL-2 and IL-15 activation in culture. We developed a 2-dimensional contact assay and used live-cell imaging to quantitate the contact area between NK cells and tumors (Fig. 2A). For these human experiments, two donors were tested with the neuroblastoma cell lines CHLA-90 and SK-N-AS, which were chosen because they exhibited comparable human leukocyte antigen expression levels (data not shown). The contact between tumor and effector cells, as well as cell death, over time were highly correlated (Spearman $r = 0.6$; $P = 0.005$; Fig. 2B and C). Although NK–neuroblastoma cell contact was predicted by time ($P < 0.001$), donor ($P < 0.001$), and tumor cell line ($P < 0.001$), it was independent of the type of cytokine stimulation ($P > 0.05$). Collectively, these results suggest that the cellular interaction of NK cells with tumors are equivalent after preactivation with IL-15 or IL-2.

IL-15 increases the number of tumor-infiltrating NK cells in neuroblastoma tumorspheres

Neuroblastoma is associated with repressed immunity, which is associated with low tumor mutational burden and reflected by a lack of infiltrating T lymphocytes in the tumor microenvironment (18–20). IL-15 promotes chemotaxis of NK cells (16) and therefore may improve tumor invasion in neuroblastoma. To study the effect of IL-15 on NK cell chemotaxis, we developed a PDX tumorsphere model using the “immune cold” PDX line SJNBL046_X that, despite visible splenic infiltration, lacks the presence of tumor-infiltrating immune cells in a humanized mouse model (Fig. 3A). Initially, we isolated NK cells from the peripheral blood of healthy donors and quantitated the number of IL-15–activated NK cells in the tumorspheres. Sphere-infiltrating NK cells (SPHINKs) were detectable within 4 hours of incubation (Fig. 3B) and upregulated cell surface expression of NKp44, CD69, CD25, and CD56, as compared with NK cells that were co-cultured with but did not infiltrate tumor spheres (Fig. 3C). However, we found that FACS-isolated SPHINKs eliminated significantly less K562 tumor cells in culture than did sphere-associated NK cells ($P \leq 0.001$), suggesting an attenuated cytotoxic capacity (Fig. 3D). Determining the expression of exhaustion markers, we noted comparable percentages of PD-1, TIM-3, and LAG-3 expression. However, a higher percentage of SPHINKs expressed TIGIT than did tumorsphere non-infiltrating NK cells (supplementary figure 1). We compared the chemotactic effects of IL-15 with those of IL-2 and detected higher numbers of SPHINKs after prestimulation with IL-15 ($P = 0.002$; Fig. 3E). Taken together, This PDX-derived spheroid neuroblastoma model recapitulates the immunosuppressive tumor microenvironment and attenuates NK cell function despite compensatory upregulation of activating NK cell receptors. We demonstrated that IL-15 can partially overcome these barriers by increasing NK cell invasion into tumors in this model.

Monoclonal antibody therapy combined with the IL-15/IL-15Rα complex controls tumor growth of neuroblastoma PDXs *in vivo*

Preclinical studies have demonstrated enhanced ADCC in the presence of IL-15 (7–9). Therefore, we integrated the IL-15/IL-15Rα complex into a treatment regimen that is closely aligned with the chemoimmunotherapy regimen given to patients in the clinic (21, 22) and

tested whether IL-15 can substitute for IL-2 in immunotherapy for neuroblastoma. We evaluated the antitumor effects in four experimental groups with PDX-bearing CD1-*Foxn1*^{nu} mice (Fig. 4A), which are immunocompromised and have decreased numbers but fully functional endogenous NK cells with xenoreactivity (Supplementary Fig. S2) (23). Before proceeding with the experiment, we also examined whether immune editing occurred when human PDX cells were propagated in nude mice instead of more immunocompromised NSG mice. We injected 1×10^6 SJNBL046_X neuroblastoma xenograft cells orthotopically into nude and NSG mice. These tumors grew within 4-5 weeks and were subsequently processed into a single-cell suspension and analyzed for NK cell ligands. We then used residual tumor cells and re-injected them into mice, switching the host (i.e., tumor harvested from nude mouse was reinjected into an NSG mouse and vice versa). After about 4-5 weeks, tumor growth was apparent by ultrasound and the analysis for NK cell ligands was repeated. NK cell ligands did not change expression when tumors from NSG mice were passaged through nude mice (e.g., ULBP2, DR4, CD112, MICA, and MICB) or vice versa (e.g., DR4, DR5, CD112, ULBP3, MICA, and MICB; Supplementary Fig. 3). There were other ligands that were downregulated. However, downregulation was noted in both sub-sets of experiments (e.g., NTB-A and CD155), suggesting that this was not due to host-related immune editing.

Mice received chemotherapy alone (group 1); chemotherapy followed by 14.G2a antibody and GM-CSF (group 2); chemotherapy followed by 14.G2a antibody, GM-CSF, and IL-2 (group 3); or chemotherapy followed by 14.G2a antibody, GM-CSF, and IL-15/IL-15Rα complex (group 4; Fig. 4B). Weekly tumor volumes and weights (Supplementary Fig. S4) were obtained.

Animals in group 4 exhibited the most suppressed tumor growth among all four therapy groups (Fig. 4C). In direct comparison, mice in group 4 had smaller tumors than those in group 1 ($P = 0.011$), group 2 ($P = 0.016$), and group 3 ($P = 0.035$). 5 of 7 (71%) mice in group 4 achieved partial (> 20% volume reduction) or complete tumor regression, whereas tumor regression did not occur in any group 1 mice (0/8; 0%), occurred in three in group 2 (3/6; 50%), and occurred in one in group 3 (1/7; 14%; Fig. 4D). None of the mice did lost more than 20% of their body weight during therapy, demonstrating tolerability of the chemoimmunotherapy regimens (Supplementary Fig. S4). Altogether, we found that the substitution of IL-15/IL-15Rα for IL-2 leads to significantly improved tumor regression *in vivo*.

IL-15/IL-15Rα increases the proportion of mature NK cells in tumors and up-regulates *Gzmd* expression in vitro

In animals that completed therapy, we harvested the spleens and tumors (if present) to analyze the proportions of tissue-infiltrating monocytes/macrophages and NK cells. By using a gating strategy as previously described (24), we quantitated the percentage of CD11b$^+$ Ly6G$^-$Ly6C$^+$MHC II$^-$ (monocytes) and CD11b$^+$ Ly6G$^-$Ly6C$^-$MHC II$^+$ tumor-associated macrophages and used the spleen as a reference (Fig. 5A). Generally, higher percentages of CD11b$^+$ Ly6G$^-$ macrophages were found in tumors than in spleens for all therapy groups, except group 2 (Fig. 5B). These macrophages primarily comprised a CD11b$^+$Ly6G$^-$Ly6C$^-$MHC II$^+$ population (Fig. 5C and D). When we quantified the percentage of

$DX5^+CD27^+CD11b^-$ immature NK cells and $DX5^+CD27^-CD11b^+$ mature NK cells in tumors and spleens (25) (Fig. 5E), we did not find any significant differences between the NK cell percentages in the two tissues or within tissues among the different therapy groups (Fig. 5F). However, we observed significantly decreased numbers of $DX5^+CD27^+$ immature NK cells in tumors from mice treated with the IL-15/IL-15Rα complex than in other therapy groups ($P = 0.012$), whereas no difference was noted in spleens (Fig. 5F and G). This suggests that IL-15/IL-15Rα promotes NK cell maturation, thereby decreasing the proportions of immature tumor-infiltrating NK cells.

To investigate transcriptional changes and activation of functional pathways leading to enhanced cytotoxicity of NK cells after IL-15 stimulation compared to IL-2, we performed differential gene expression of NK cells from CD1-*Foxn1*^{nu} mice after stimulation with either cytokine. Analyzing bulk RNA sequencing data of two experimental replicates for each condition, we noted that IL-15 activation led to a 117-fold (or 6.9-log fold) upregulation of *Gzmd* compared to IL-2 (Supplementary Fig. S5). Granzyme D is expressed in murine cytotoxic lymphocytes and functionally homologous to human granzyme B or H (26). Thus, an elevated expression of *Gzmd* could contribute to the enhanced anti-tumor activity observed in IL-15-compared to IL-2-treated mice.

Discussion

A seminal immunotherapy trial in pediatric solid tumors established the efficacy of an anti-GD2 antibody, IL-2, and GM-CSF for neuroblastoma (3). Although this regimen is now the standard of care, treatment failure and IL-2-related toxicities remain a clinical challenge. Because of the known biologic effects of IL-15 on NK cell function and development, we investigated the immunoadjuvant properties of IL-15 in the context of neuroblastoma immunotherapy. We found that IL-15, integrated in the current immunotherapy regimen for neuroblastoma, exhibits notable preclinical antitumor activity *in vitro* and *in vivo* that exceeds the effect of IL-2 in a murine model with established tumors. The anti-tumor effect of immunotherapy with IL-2 *in vivo* was comparable to tumor shrinkage induced by chemotherapy with or without antibody and GM-CSF. Although this observation appears to be at odds with the current treatment consensus, it is important to point out that immunotherapy with anti-GD2 antibody, IL-2, and GM-CSF has proven to be effective in the state of minimal residual disease (28). There is emerging evidence that the combination of chemo-immunotherapy also induces shrinkage of large tumors in the clinic (2). However, studies of chemo-immunotherapy in an established xenograft model have not been performed prior to our report. Based on these findings, we propose that IL-15 is a feasible substitute for IL-2 and should be included in future clinical studies to test the tolerability of IL-15 for immunotherapy in children with relapsed/refractory neuroblastoma, with antitumor effects as a secondary endpoint.

Recombinant IL-2 was the first cytokine used in the clinic for cancer therapy (27). However, the therapeutic benefit of IL-2 for high-risk neuroblastoma is controversial. In the most recent randomized controlled trial by the European SIOP Neuroblastoma Group, there was no survival benefit at 3 years with the addition of subcutaneous (SC) high-dose IL-2 (6×10^6 IU/m2 per day for 10 days) to ch14.18/CHO and GM-CSF. Nevertheless, cautious

interpretation of these results is warranted given that one-third of patients abrogated therapy due to IL-2–related toxicities, thus confounding the study results (28). Low or ultralow doses of IL-2 are better tolerated but can induce regulatory T cell proliferation, which suppresses NK cell expansion and function in preclinical studies (29).

IL-15 has unique pharmacokinetic, can directly engage IL2Rβγ, and requires IL-15Rα to form a complex for trans-presentation on the cell surface of activated monocytes to exert its immunologic properties (30). In the presence of GM-CSF, IL-15 is mobilized to the plasma membrane of monocytes (31), which may increase its bioavailability. Patients with neuroblastoma receive GM-CSF because it improves ADCC in preclinical studies (32). Therefore, by replacing IL-2 with IL-15 in the current therapy regimen, this effect may be further exploited, leading to a reduction in overall cytokine doses required for inducing the desired biologic antitumor effects and improve the tolerability of chemoimmunotherapy.

The IL-15 and IL-15Rα concentrations used in our in vivo experiments were based on previously published dosing in mice that yielded a biologic effect in NK cells (15). In preclinical studies with ALT-803, an IL-15/IL-15Rα complex, mice received 0.2 mg/kg of ALT-803 on day 1 and 8 of therapy that corresponds to 0.06 mg/kg of IL-15 (33). We administered IL-15 at a dose of about 0.08 mg/kg on day 8 of each cycle. Therefore, we believe that the chosen regimen is in the range of previously tested in vivo concentrations that in case of ALT-803 were successfully translated into the clinic.

Recombinant human IL-15 has been tested as intravenous (IV) bolus infusion (10) and SC injection (34) in adult patients with cancer. The maximum tolerated dose was found to be significantly lower when given as IV bolus infusion (0.3 μg/kg/day) than as SC injection (2.0 μg/kg/day). Grade 3 or 4 adverse events at these dose levels were reported to be AST elevation, leukopenia, lymphopenia, neutropenia, and anemia (IV) as well as hypophosphatemia, hypertension, and lymphopenia (SC), respectively. In patients who received IL-15 daily by bolus infusion for 12 consecutive days, correlative analysis of NK cell kinetics in the peripheral blood revealed decreased cell numbers as early as 20 minutes after start of the infusion, influx or demarginalization of NK cells over the subsequent 2 days, followed by hyperproliferation until daily infusions were ceased (10). In patient who underwent daily SC injections of IL-15 for 5 days of two consecutive weeks, highest NK cell numbers were found 3 days after completion of this regimen (day 15). However, cytotoxicity against K562 was higher after the 10^{th} dose of IL-15 compared pretreatment and day 15 testing (34). Considering this knowledge regarding NK cell function, NK cell expansion, and spectrum of adverse events with IL-15 treatment, there are several ways to incorporate either IV or SC IL-15 after confirming the pharmacokinetic and dynamic data obtained in adults in a pediatric phase I trial. For example, one could administer daily IV IL-15 and start anti-GD2 antibody and GM-CSF on day 3-7. Alternatively, adopting the SC injection regimen, patients may be pre-treated with 5 days of SC IL-15 and commence anti-GD2 antibody and GM-CSF therapy during week 2 (day 8-12).Cytokine-producing $CD56^{bright}$ NK cells are hypothesized to be the precursors of terminally differentiated cytotoxic $CD56^{dim}$ NK cells (35) and to mature in response to IL-15 (36). However, the predominant subtype in tumors comprise $CD56^{bright}$-infiltrating NK cells (37). In our study, the number of immature murine $CD27^{+}CD11b^{-}$ NK cells decreased more in tumors after

treatment with IL-15 than with other therapy groups, constituting a potential mechanism for improved ADCC with IL-15. This should be confirmed with more detailed phenotypic characterization, such as CD16 expression, in the future.

In this study, we used athymic immunocompromised CD1-*Foxn1*^{nu} mice that have low numbers of functional NK cells. We performed phenotypic, cytotoxic, and molecular studies to assess the functionality of NK cells derived from these animals. NK cells produced interferon-γ, perforin, and granzyme B, and were able to degranulate upon contact with target cells. In addition, they showed significant upregulation of *Gzmd* and activation of the granzyme A pathway that corresponded to increased cytotoxicity and cytokine production after activation with IL-15 in culture. Altogether these findings suggest that NK cells from CD1-*Foxn1*^{nu} mice can execute common NK cell functions and respond accordingly to stimulation with IL-2 and IL-15.

Paradoxically, we found increased tumorsphere invasion by IL-15-activated NK cells but less cytotoxic efficacy in these cells compared to tumor-non-infiltrating NK cells. We hypothesized that this effect may be induced by the immune-suppressive tumor microenvironment. Compared to resting NK cells, we found that IL-2 and IL-15 activation can partially preserve the cytotoxic function of tumorsphere-infiltrating NK cells.

Although nude mice have been previously utilized to model ADCC in neuroblastoma and led to the discovery of the monoclonal anti-GD2 antibody for therapeutic purposes (38), there are several limitations to this model system. The passaging of tumor cells in nude mice did not results in immune sculpting of common NK cell ligands. However, in our ex vivo experiments, we noted significantly less NK cell cytotoxicity against human than mouse tumor cells. In the presence of anti-GD2 antibody, lysis of human neuroblastoma PDX cells by IL-15-activated murine NK cells approximated that yielded by resting murine NK cells against the syngeneic cell line YAC-1. Although NK cells have been regarded as one of the primary effector population in ADCC, it is unclear to what degree murine myeloid cells contributed to tumor shrinkage in our experiments. Nevertheless, the combined effect of myeloid and NK cells led to significant tumor shrinkage in our tumor model when IL-2 was replaced by IL-15 in the current immunotherapy regimen. Future studies could further clarify the relative contribution of myeloid cells by using clodronate or other agents that temporarily decrease the number of this population (39). Likewise, the use of anti-GM1 antibody that neutralizes murine NK cells could help discern the cytotoxic effect of NK cells (40). Other limitations are the use of only one PDX line in the tumorsphere model.

Based on our results, we propose that recombinant human IL-15 or the soluble IL-15/IL-15Rα complex is a feasible IL-2 substitute in the current immunotherapy regimen for neuroblastoma. Because IL-15 has not been previously tested in pediatric studies, initial efforts to evaluate its tolerability in children should be prioritized but reports of tumor responses as a secondary endpoint should be included, in addition to detailed correlative studies to elucidate the biologic effects of IL-15 when given in combination with immunotherapy.

Supplementary Material

Refer to Web version on PubMed Central for supplementary material.

Acknowledgments

We thank Asa Karlstrom, PhD, for regulatory support; Nisha Badders, PhD, ELS, for editing the manuscript; Jennifer Peters, PhD, for optimizing the live-cell microscopy protocol; Melissa Johnson, BS, for performing tumor injections; Benjamin Youngblood, PhD, for comments and suggestions; Merck Serono and Children's GMP, LLC for providing hu14.18K322A for our studies; and the NCI Biological Resource Branch for providing IL-2 and IL-15.

This work was supported by the National Institutes of Health grant P30 CA021765 and ALSAC (all authors); ASCO Conquer Cancer Young Investigator Award (12822; RN); R50CA211481 (WJA); EY014867, EY018599, and CA168875 (MAD). This research was supported by HHMI.

Abbreviations:

ADCC	antibody-dependent cell-mediated cytotoxicity
E:T	effector-to-target
FACS	fluorescence-activated cell sorting
GD2	disialoganglioside
GM-CSF	granulocyte-macrophage colony-stimulating factor
IL-15	interleukin 15
IL-2	interleukin 2
IL2Rβγ	IL2 receptor βγ
IV	intravenous
NK	natural killer
PDXs	patient-derived xenografts
RLU	relative light units
SC	subcutaneous
SPHINKs	sphere-infiltrating NK cells
YFP	yellow fluorescent protein

References

1. Ries LS MA; Gurney JG; Linet M; Tamra T; Young JL; Bunin GR. Cancer Incidence and Survival among Children and Adolescents: United States SEER Program 197-1995. Bethesda, MD: National Cancer Institute; 1999 Report No.: NIH Pub. No. 99-4649.
2. Allavena P, Giardina G, Bianchi G, Mantovani A. IL-15 is chemotactic for natural killer cells and stimulates their adhesion to vascular endothelium. J Leukoc Biol. 1997;61(6):729–35. [PubMed: 9201264]

3. Arganda-Carreras I, Kaynig V, Rueden C, Eliceiri KW, Schindelin J, Cardona A, et al. Trainable Weka Segmentation: a machine learning tool for microscopy pixel classification. Bioinformatics. 2017;33(15):2424–6. [PubMed: 28369169]
4. Chiossone L, Chaix J, Fuseri N, Roth C, Vivier E, Walzer T. Maturation of mouse NK cells is a 4-stage developmental program. Blood. 2009;113(22):5488–96. [PubMed: 19234143]
5. Conlon KC, Lugli E, Welles HC, Rosenberg SA, Fojo AT, Morris JC, et al. Redistribution, hyperproliferation, activation of natural killer cells and CD8 T cells, and cytokine production during first-in-human clinical trial of recombinant human interleukin-15 in patients with cancer. J Clin Oncol. 2015;33(1):74–82. [PubMed: 25403209]
6. Dubois S, Mariner J, Waldmann TA, Tagaya Y. IL-15Ralpha recycles and presents IL-15 In trans to neighboring cells. Immunity. 2002;17(5):537–47. [PubMed: 12433361]
7. Federico SM, McCarville MB, Shulkin BL, Sondel PM, Hank JA, Hutson P, et al. A Pilot Trial of Humanized Anti-GD2 Monoclonal Antibody (hu14.18K322A) with Chemotherapy and Natural Killer Cells in Children with Recurrent/Refractory Neuroblastoma. Clin Cancer Res. 2017;23(21): 6441–9. [PubMed: 28939747]
8. Fellows E, Gil-Parrado S, Jenne DE, Kurschus FC. Natural killer cell-derived human granzyme H induces an alternative, caspase-independent cell-death program. Blood. 2007;110(2):544–52. [PubMed: 17409270]
9. Fogh J The Nude Mouse in Experimental and Clinical Research: Elsevier Science; 2014.
10. Ghiringhelli F, Menard C, Terme M, Flament C, Taieb J, Chaput N, et al. CD4+CD25+ regulatory T cells inhibit natural killer cell functions in a transforming growth factor-beta-dependent manner. J Exp Med. 2005;202(8):1075–85. [PubMed: 16230475]
11. Giri JG, Ahdieh M, Eisenman J, Shanebeck K, Grabstein K, Kumaki S, et al. Utilization of the beta and gamma chains of the IL-2 receptor by the novel cytokine IL-15. EMBO J. 1994;13(12):2822–30. [PubMed: 8026467]
12. Hank JA, Robinson RR, Surfus J, Mueller BM, Reisfeld RA, Cheung NK, et al. Augmentation of antibody dependent cell mediated cytotoxicity following in vivo therapy with recombinant interleukin 2. Cancer Res. 1990;50(17):5234–9. [PubMed: 2386933]
13. Hwang WL, Wolfson RL, Niemierko A, Marcus KJ, DuBois SG, Haas-Kogan D. Clinical Impact of Tumor Mutational Burden in Neuroblastoma. J Natl Cancer Inst. 2018.
14. Kratochvill F, Neale G, Haverkamp JM, Van de Velde LA, Smith AM, Kawauchi D, et al. TNF Counterbalances the Emergence of M2 Tumor Macrophages. Cell Rep. 2015;12(11):1902–14. [PubMed: 26365184]
15. Ladenstein R, Potschger U, Valteau-Couanet D, Luksch R, Castel V, Yaniv I, et al. Interleukin 2 with anti-GD2 antibody ch14.18/CHO (dinutuximab beta) in patients with high-risk neuroblastoma (HR-NBL1/SIOPEN): a multicentre, randomised, phase 3 trial. Lancet Oncol. 2018;19(12):1617–29. [PubMed: 30442501]
16. Lanier LL, Le AM, Civin CI, Loken MR, Phillips JH. The relationship of CD16 (Leu-11) and Leu-19 (NKH-1) antigen expression on human peripheral blood NK cells and cytotoxic T lymphocytes. J Immunol. 1986;136(12):4480–6. [PubMed: 3086432]
17. Levi I, Amsalem H, Nissan A, Darash-Yahana M, Peretz T, Mandelboim O, et al. Characterization of tumor infiltrating natural killer cell subset. Oncotarget. 2015;6(15):13835–43. [PubMed: 26079948]
18. Lin JX, Du N, Li P, Kazemian M, Gebregiorgis T, Spolski R, et al. Critical functions for STAT5 tetramers in the maturation and survival of natural killer cells. Nat Commun. 2017;8(1):1320. [PubMed: 29105654]
19. Matthay KK, Villablanca JG, Seeger RC, Stram DO, Harris RE, Ramsay NK, et al. Treatment of high-risk neuroblastoma with intensive chemotherapy, radiotherapy, autologous bone marrow transplantation, and 13-cis-retinoic acid. Children's Cancer Group. N Engl J Med. 1999;341(16): 1165–73. [PubMed: 10519894]
20. Miller JS, Morishima C, McNeel DG, Patel MR, Kohrt HEK, Thompson JA, et al. A First-in-Human Phase I Study of Subcutaneous Outpatient Recombinant Human IL15 (rhIL15) in Adults with Advanced Solid Tumors. Clin Cancer Res. 2018;24(7):1525–35. [PubMed: 29203590]

21. Mody R, Naranjo A, Van Ryn C, Yu AL, London WB, Shulkin BL, et al. Irinotecan-temozolomide with temsirolimus or dinutuximab in children with refractory or relapsed neuroblastoma (COG ANBL1221): an open-label, randomised, phase 2 trial. Lancet Oncol. 2017;18(7):946–57. [PubMed: 28549783]
22. Moga E, Alvarez E, Canto E, Vidal S, Rodriguez-Sanchez JL, Sierra J, et al. NK cells stimulated with IL-15 or CpG ODN enhance rituximab-dependent cellular cytotoxicity against B-cell lymphoma. Exp Hematol. 2008;36(1):69–77. [PubMed: 17959301]
23. Mujoo K, Cheresh DA, Yang HM, Reisfeld RA. Disialoganglioside GD2 on human neuroblastoma cells: target antigen for monoclonal antibody-mediated cytolysis and suppression of tumor growth. Cancer Res. 1987;47(4):1098–104. [PubMed: 3100030]
24. Neely GG, Robbins SM, Amankwah EK, Epelman S, Wong H, Spurrell JC, et al. Lipopolysaccharide-stimulated or granulocyte-macrophage colony-stimulating factor-stimulated monocytes rapidly express biologically active IL-15 on their cell surface independent of new protein synthesis. J Immunol. 2001;167(9):5011–7. [PubMed: 11673509]
25. Nguyen QH, Roberts RL, Ank BJ, Lin SJ, Thomas EK, Stiehm ER. Interleukin (IL)-15 enhances antibody-dependent cellular cytotoxicity and natural killer activity in neonatal cells. Cell Immunol. 1998;185(2):83–92. [PubMed: 9636686]
26. Nguyen R, Houston J, Chan WK, Finkelstein D, Dyer MA. The role of interleukin-2, all-trans retinoic acid, and natural killer cells: surveillance mechanisms in anti-GD2 antibody therapy in neuroblastoma. Cancer Immunol Immunother. 2018;67(4):615–26. [PubMed: 29327110]
27. Ollion J, Cochennec J, Loll F, Escude C, Boudier T. TANGO: a generic tool for high-throughput 3D image analysis for studying nuclear organization. Bioinformatics. 2013;29(14):1840–1. [PubMed: 23681123]
28. Pugh TJ, Morozova O, Attiyeh EF, Asgharzadeh S, Wei JS, Auclair D, et al. The genetic landscape of high-risk neuroblastoma. Nat Genet. 2013;45(3):279–84. [PubMed: 23334666]
29. Rhode PR, Egan JO, Xu W, Hong H, Webb GM, Chen X, et al. Comparison of the Superagonist Complex, ALT-803, to IL15 as Cancer Immunotherapeutics in Animal Models. Cancer Immunol Res. 2016;4(1):49–60. [PubMed: 26511282]
30. Ribeiro RC, Rill D, Roberson PK, Furman WL, Pratt CB, Brenner M, et al. Continuous infusion of interleukin-2 in children with refractory malignancies. Cancer. 1993;72(2):623–8. [PubMed: 8319196]
31. Rosenberg SA, Lotze MT, Muul LM, Leitman S, Chang AE, Ettinghausen SE, et al. Observations on the systemic administration of autologous lymphokine-activated killer cells and recombinant interleukin-2 to patients with metastatic cancer. N Engl J Med. 1985;313(23):1485–92. [PubMed: 3903508]
32. Schindelin J, Arganda-Carreras I, Frise E, Kaynig V, Longair M, Pietzsch T, et al. Fiji: an open-source platform for biological-image analysis. Nat Methods. 2012;9(7):676–82. [PubMed: 22743772]
33. Sechler JM, Barlic J, Grivel JC, Murphy PM. IL-15 alters expression and function of the chemokine receptor CX3CR1 in human NK cells. Cell Immunol. 2004;230(2):99–108. [PubMed: 15598425]
34. Stewart E, Shelat A, Bradley C, Chen X, Federico S, Thiagarajan S, et al. Development and characterization of a human orthotopic neuroblastoma xenograft. Dev Biol. 2015;407(2):344–55. [PubMed: 25863122]
35. Stoklasek TA, Schluns KS, Lefrancois L. Combined IL-15/IL-15Ralpha immunotherapy maximizes IL-15 activity in vivo. J Immunol. 2006;177(9):6072–80. [PubMed: 17056533]
36. Vincent M, Bessard A, Cochonneau D, Teppaz G, Sole V, Maillasson M, et al. Tumor targeting of the IL-15 superagonist RLI by an anti-GD2 antibody strongly enhances its antitumor potency. Int J Cancer. 2013;133(3):757–65. [PubMed: 23354868]
37. Yang RK, Kalogriopoulos NA, Rakhmilevich AL, Ranheim EA, Seo S, Kim K, et al. Intratumoral hu14.18-IL-2 (IC) induces local and systemic antitumor effects that involve both activated T and NK cells as well as enhanced IC retention. J Immunol. 2012;189(5):2656–64. [PubMed: 22844125]

38. Yu AL, Gilman AL, Ozkaynak MF, London WB, Kreissman SG, Chen HX, et al. Anti-GD2 antibody with GM-CSF, interleukin-2, and isotretinoin for neuroblastoma. N Engl J Med. 2010;363(14):1324–34. [PubMed: 20879881]

39. Zhang M, Wen B, Anton OM, Yao Z, Dubois S, Ju W, et al. IL-15 enhanced antibody-dependent cellular cytotoxicity mediated by NK cells and macrophages. Proc Natl Acad Sci U S A. 2018;115(46):E10915–E24. [PubMed: 30373815]

40. Zhang P, Wu X, Basu M, Dong C, Zheng P, Liu Y, et al. MYCN Amplification Is Associated with Repressed Cellular Immunity in Neuroblastoma: An In Silico Immunological Analysis of TARGET Database. Front Immunol. 2017;8:1473. [PubMed: 29163537]

Translational Relevance

Combinatorial immunotherapy with interleukin (IL)-2, granulocyte-macrophage colony-stimulating factor, and a monoclonal antibody against disialoganglioside improves event-free survival in children with high-risk neuroblastoma. The antitumor effects of this therapy are executed by natural killer (NK) cells via antibody-dependent cell-mediated cytotoxicity (ADCC). However, one-third of the patients experience treatment failure, and many children suffer from acute IL-2–related toxicities. To evaluate alternative cytokines for immunotherapy in neuroblastoma, we compared the immunoadjuvant effects of a complexed form of IL-15, a known stimulatory cytokine with specific effects on NK cell development and function, with those of IL-2. Substitution of IL-15/IL-15Rα for IL-2 enhanced ADCC against patient-derived neuroblastoma xenografts *in vitro* and in mice. Enhanced *in vivo* ADCC most likely occurred because IL-15 promoted maturation of tumor-infiltrating NK cells. These results demonstrate that IL-15 is more effective than IL-2 for enhancing ADCC against neuroblastoma and support clinical testing of IL-15 for immunotherapy in pediatric neuroblastoma.

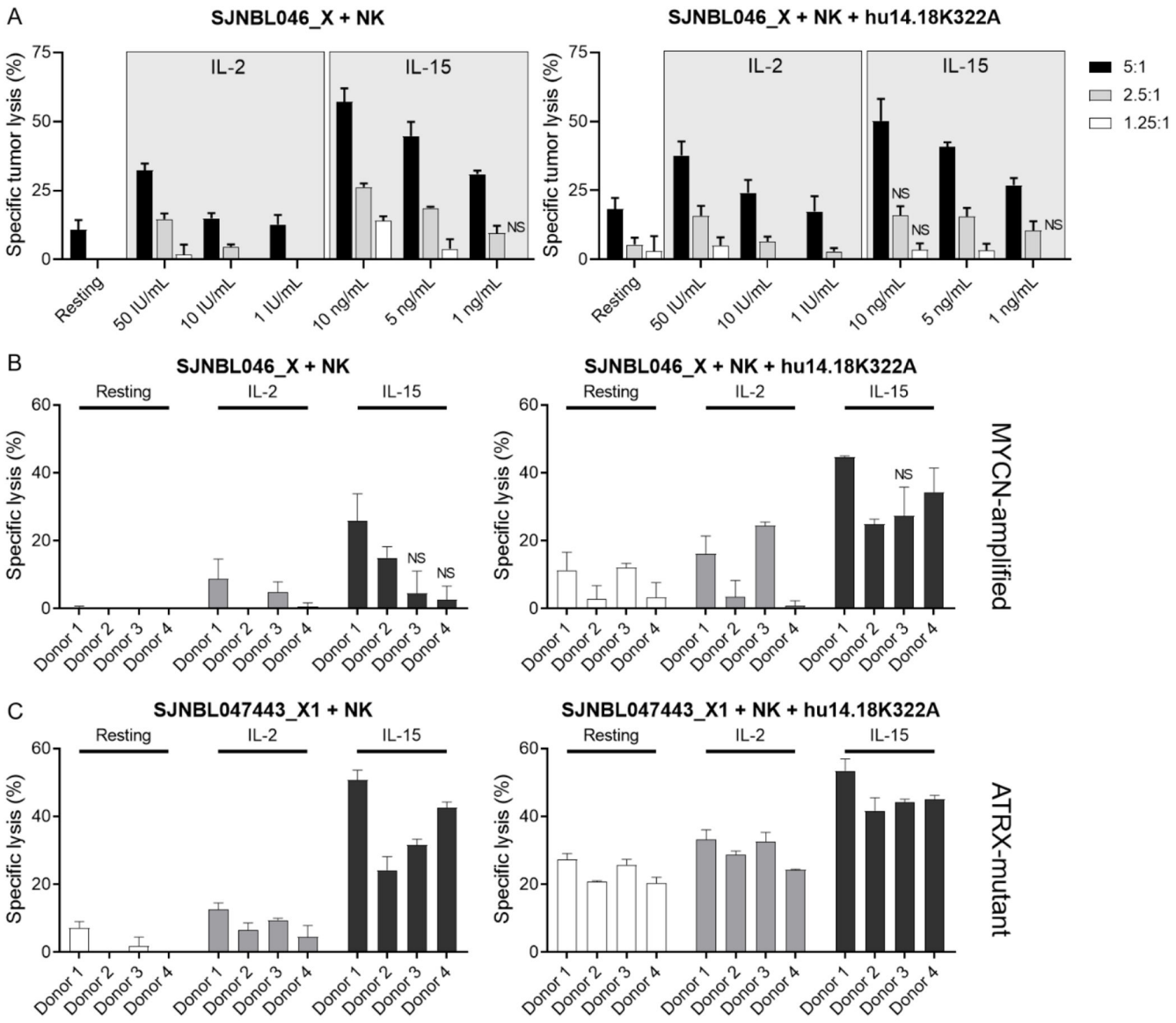

Figure 1.

Immunoadjuvant effects of IL-15 and IL-2 on NK cell cytotoxicity and ADCC against neuroblastoma. **A,** NK cells were prestimulated with several concentrations of IL-2 and IL-15 for 24 hours and subsequently tested with the PDX SJNBL046_X at different E:T ratios. The assays were conducted with NK cells from two donors, with and without hu14.18K322A. All experiments were performed in technical quadruplets and mean tumor lysis and standard deviation were plotted. Tumor lysis by IL-15-activated NK cells was significantly greater than that of IL-2-activated NK cells, except in the marked conditions (NS). **B** and **C,** NK cells from four donors were tested against the two PDX lines PDX SJNBL046_X (**B**) and SJNBL047443_X1 (**C**), with an E:T ratio of 5:1 and intermediate concentrations of IL-2 (10 IU/mL) and IL-15 (5 ng/mL). IL-15–preactivated NK cells induced higher cytolysis when directly compared with that of IL-2–activated NK cells. This

was noted in presence and absence of an anti-GD2 antibody. Exceptions are marked accordingly (NS).

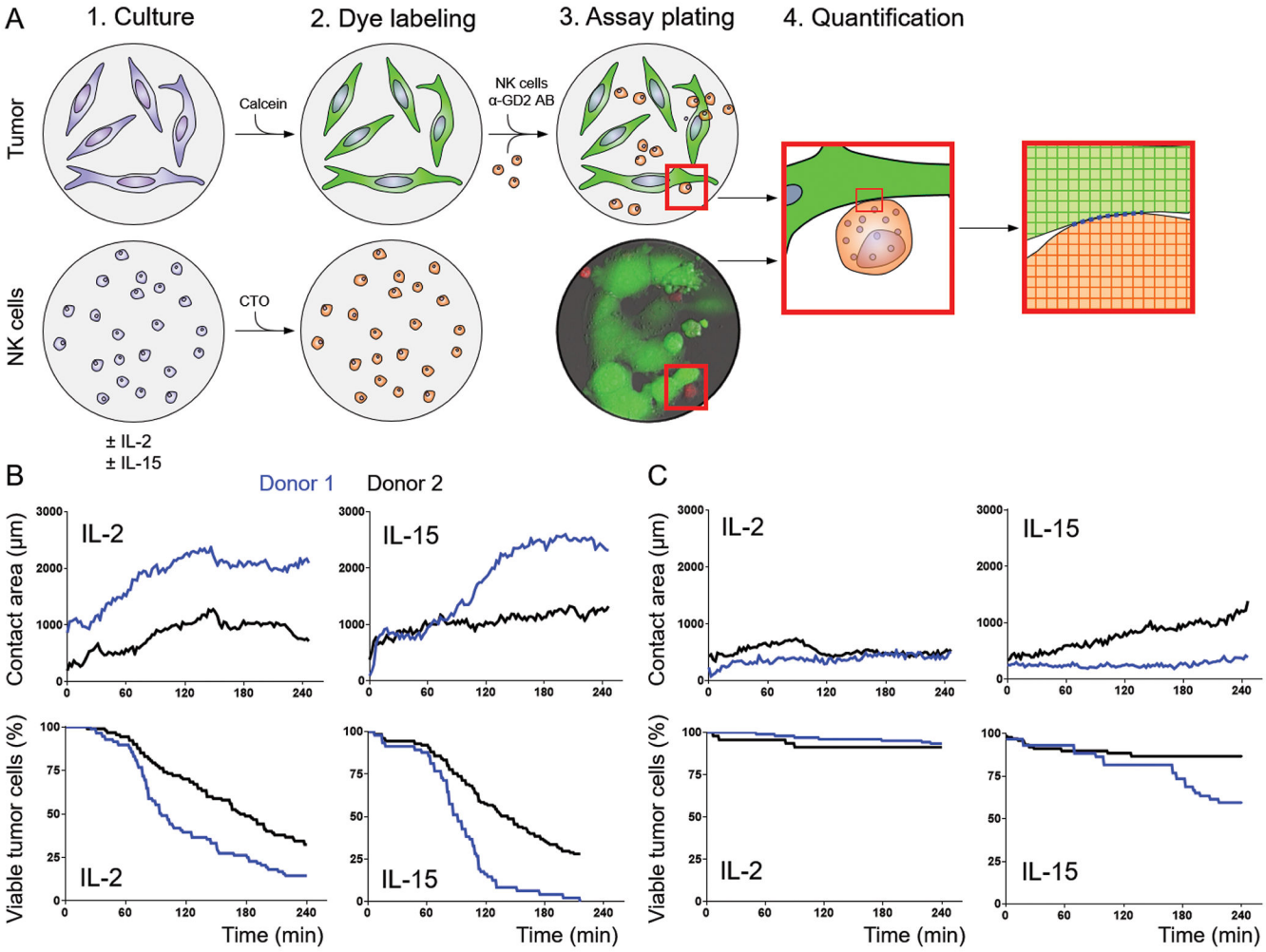

Figure 2.

Quantification of NK cell–neuroblastoma contact. **A,** One day before the assay, NK cells were grown in culture in NK cell media supplemented with IL-2 or IL-15, and neuroblastoma cells were plated. On the day of the assay, neuroblastoma cells were labeled with calcein-AM, and NK cells were labeled with CellTracker Orange. Hu14.18K322A and dye-labeled NK cells were added to the wells, and the contact between neuroblastoma cells and NK cells was imaged and later quantitated in silico. Five different areas were imaged per condition and the mean is plotted per time point. **B** and **C,** The assay was conducted with NK cells from two allogeneic donors and the two neuroblastoma cell lines CHLA-90 (**B**) and SK-N-AS (**C**). The normalized contact area and relative percentage of viable tumor cells are plotted over time for IL-2– and IL-15–activated NK cells from two donors (donor 1 = blue, donor 2 = black).

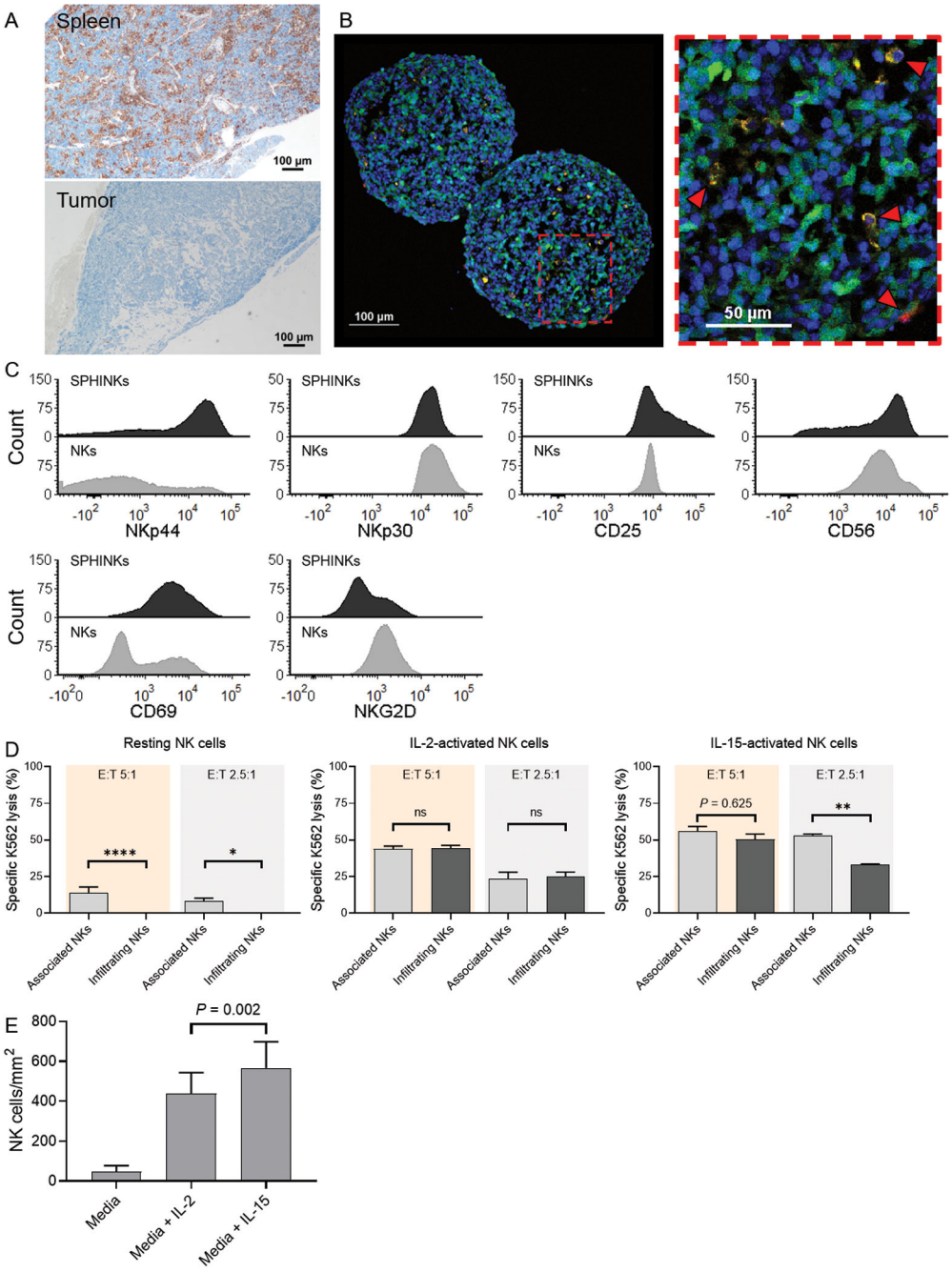

Figure 3.

Phenotype and function of sphere-infiltrating NK cells (SPHINKs). **A,** *In vivo* infiltration of spleen by adoptively transferred IL-15–activated NK cells in NOD-SCID $IL2R\gamma^{null}$ mice. Immunohistochemistry staining for human CD45 is shown. In the same animal, IL-15–activated NK cells did not infiltrate the tumor microenvironment (SJNBL046_X) **B,** YFP-expressing PDX cells (green) were used to form tumorspheres. IL-15–activated NK cells (orange) are capable of infiltrating tumorspheres (red arrows) as early as 4 hours after the assay start. DAPI staining was performed for nuclear discrimination (blue). Experiments

were performed with two donors that yielded comparable findings. Representative results from one donor are shown. **C,** Phenotypic characterization of IL-15–activated SPHINKs and IL-15–activated noninfiltrating (i.e., tumor-associated) NK cells by flow cytometry. **D,** Resting tumorsphere-infiltrating NK cells exhibited decreased cytotoxicity against K562 than did tumorsphere-non-infiltrating NK cells. This was also noted for IL-15-activated NK cells at an E:T ratio of 2.5:1. At an E:T ratio of 5:1 and when NK cells were pre-activated with IL-2, preserved cytotoxicity was noted. The experiments were performed in technical triplicates with pooled SPHINKs from 30 tumorspheres. The mean specific lysis and standard deviation were plotted. **E,** The number of SPHINKs was higher when NK cells were activated with IL-15 than with IL-2 or media alone.

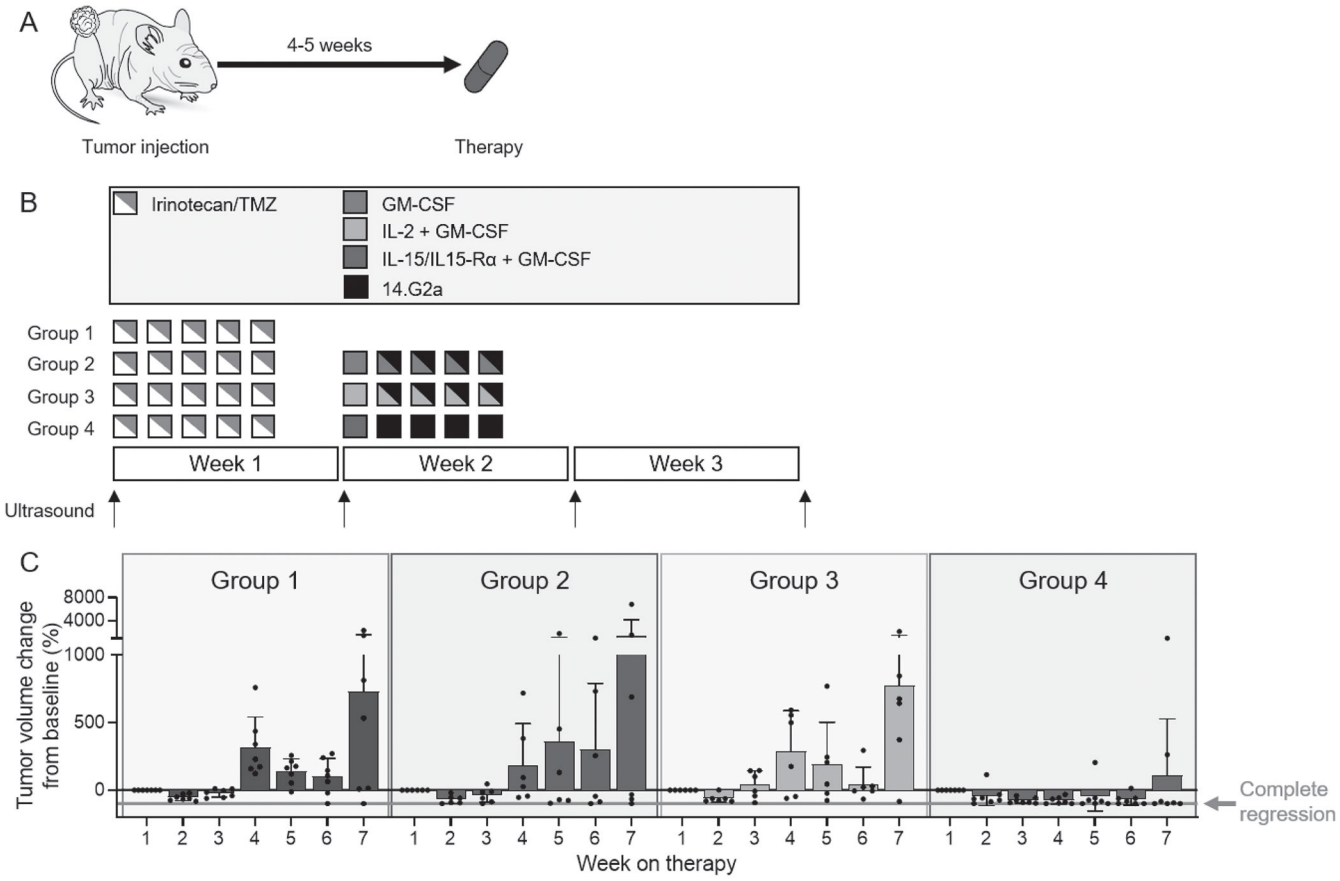

Figure 4.

Determining ADCC with IL-15/IL-15Rα in an orthotopic PDX mouse model. **A,** Nude mice aged 5 to 6 weeks were injected orthotopically with the PDX SJNBL046_X in the para-adrenal space. Four to 5 weeks after injection, mice with tumor volumes measuring ≥ 10 mm^3 by ultrasound were randomly assigned to four therapy groups. **B,** Therapy schema. Animals received two courses of therapy, each lasting 3 weeks. **C,** Median tumor growth over time in all four therapy groups. **D,** Waterfall plots showing the relative tumor volume change at the end of therapy compared to baseline measurements for individual mice in each therapy group.

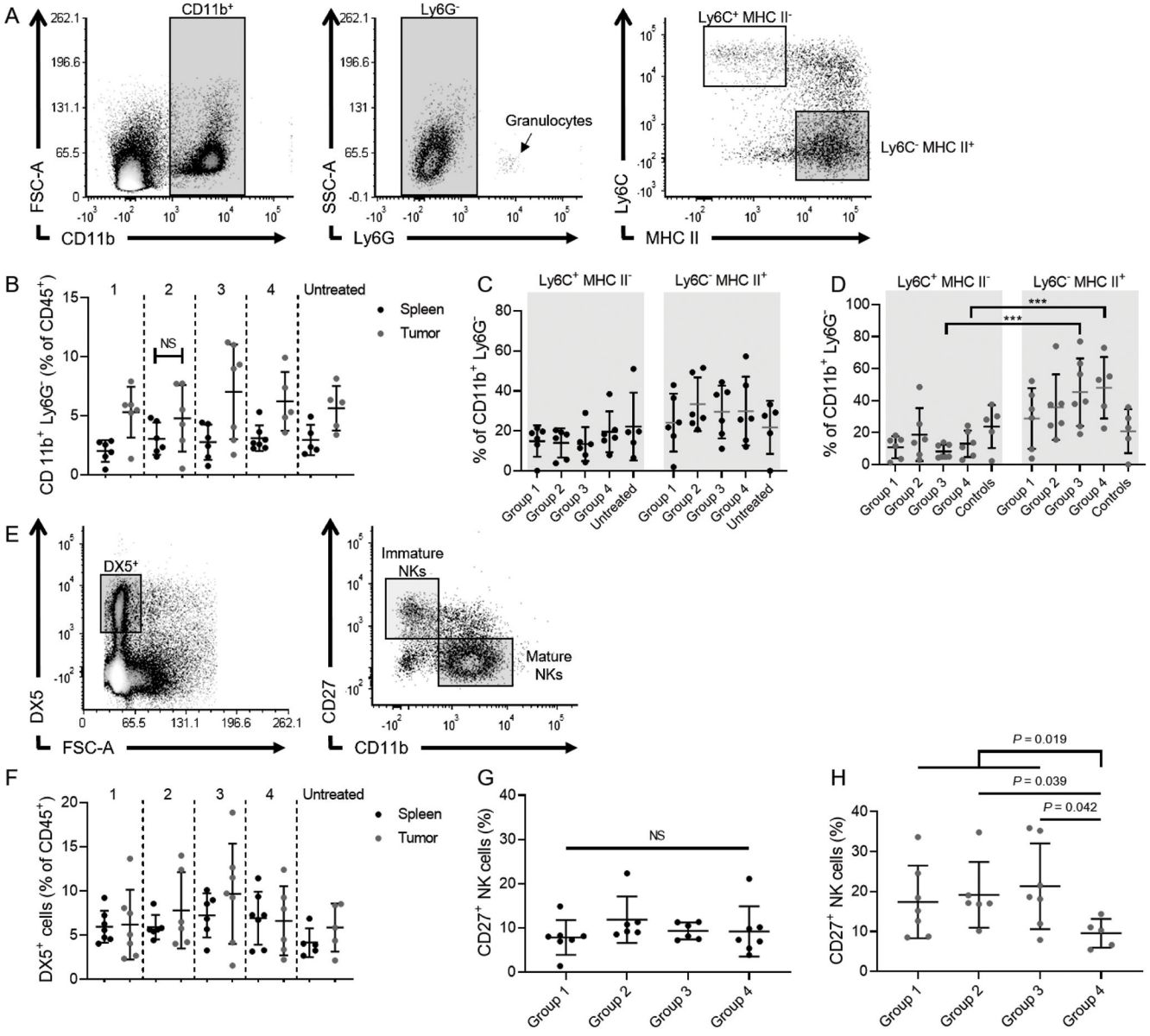

Figure 5.

Phenotype of tumor-associated macrophages/monocytes and NK cells in tumors and spleens of mice treated with chemoimmunotherapy. **A,** Gating strategy to identify $CD11b^{+}Ly6G^{-}Ly6C^{+}MHC\ II^{-}$ and $CD11b^{+}Ly6G^{-}Ly6C^{-}MHC\ II^{+}$ monocytes/macrophages. **B,** Percentage of $CD11b^{+}Ly6G^{-}$ cells of all $CD45^{+}$ cells in spleens (blue) and tumors (red). **C** and **D,** Groups refer to the assignment shown in Fig. 4B. Percentages of $CD11b^{+}Ly6G^{-}Ly6C^{+}MHC\ II^{-}$ and $CD11b^{+}Ly6G^{-}Ly6C^{-}MHC\ II^{+}$ in spleens (**C**) and tumors (**D**). **E,** Gating strategy to identify $DX5^{+}CD27^{+}CD11b^{-}$ immature NK cells and $DX5^{+}CD27^{-}CD11b^{+}$ mature NK cells. **F,** Percentage $DX5^{+}$ NK cells of all $CD45^{+}$ cells in spleens (blue) and tumors (red). **G** and **H,** Percentages of immature NK cells in spleens (**G**) and tumors (**H**).